ChemPubSoc Europe

DOI: 10.1002/cssc.201600681

CHEMSUSCHEM Full Papers

Insights into the Ring-Opening of Biomass-Derived Furanics over Carbon-Supported Ruthenium

Matthew J. Gilkey, Alexander V. Mironenko, Leerang Yang, Dionisios G. Vlachos,* and Bingjun Xu*[a]

The selective ring-opening of cellulose-derived furanic molecules is a promising pathway for the production of industrially relevant linear oxygenates, such as 1,6-hexanediol. 2,5-Dimethylfuran (DMF) is employed as a model compound in a combined experimental and computational investigation to provide insights into the metal-catalyzed ring-opening. Ring-opening to 2-hexanol and 2-hexanone and ring-saturation to 2,5-dimethyltetrahydrofuran (DMTHF) are identified as two main parallel pathways. DFT calculations and microkinetic modeling indicate that DMF adsorbs on Ru in an open-ring configuration, which is potentially a common surface intermediate that leads to both ring-opening and ring-saturation products. Although the activation barriers for the two pathways are comparable, the formation of DMTHF is more thermodynamically favorable. In addition, steric interactions with co-adsorbed 2-propoxyl, derived from the solvent, and the oxophilic nature of Ru play key roles to determine the product distribution: the former favors less bulky, that is, ring-closed, intermediates, and the latter retards O–H bond formation. Finally, we show that the hydrodeoxygenation of oxygenated furanics, such as 5-methylfurfural and (5-methyl-2-furyl)methanol, on Ru occurs preferentially at oxygen-containing side groups to form DMF, followed by either ring-opening or ring-saturation.

Introduction

Biomass is the only major source of renewable carbon, from which a variety of commodity chemicals can be produced.[1,2] The development of selective pathways for the production of platform chemicals, such as 5-hydroxymethylfurfural (HMF) and furfural, from sugars[3–5] has set the stage for their processing to industrially relevant chemicals. Typically, the upgrading of oxygenated furanics requires the selective scission of C–O bonds and saturation of relevant atoms with hydrogen, a process known as hydrodeoxygenation (HDO). The HDO of HMF has been studied extensively in the production of 2,5-dimethylfuran (DMF),[6–11] a potential fuel additive because of its high research octane number.[12] An alternative pathway from HMF entails the production of aliphatic hydrocarbons and oxygenates through selective ring-opening. This chemistry is particularly enticing for the production of diesel-range alkanes[13] or polyols,[14] for example, 1,6-hexanediol, for polymer precursors. However, the understanding of ring-opening of biomass-derived furanics is lacking.

Ring-opening directly from cyclic ethers has been conducted over bifunctional catalysts, such as supported mixed metal and metal oxides, for example, Rh-ReO_x,[15–17] Ir-ReO_x,[18] or Rh-MoO_x.[17] It was hypothesized that ring-opening occurs from saturated cyclic ethers rather than their unsaturated counterparts; thus, furfural or HMF undergo C=O bond hydrogenation and ring-saturation, followed by the opening of the fully hydrogenated furan ring. Dumesic et al. proposed that the ring-opening proceeds through the protonation of the cyclic ether by the Brønsted acidic ReO_x-H clusters.[17] The resulting carbenium ion undergoes Rh-mediated hydrogenation to form the corresponding α,ω-diol. Tomishige et al. hypothesized that ReO_x fulfills an additional role, that is, to provide a binding site for the substrate by ReO_x-mediated etherification with the hydroxyl group of the substrate.[18] Then, the ring-opened product forms through sequential protonation and hydrogenation steps. In this case, the ability of the substrate to bind through etherification reactions between the hydroxyl and ReO_x-H groups is critical to the hydrogenolysis activity. Tuteja et al. attempted to open the furan ring of HMF over an acidic zirconia phosphate supported Pd catalyst; however, various side products formed.[14] The carbonyl and hydroxymethyl groups in furfural and HMF are reactive under HDO conditions and can inflict selectivity challenges, which favors side reactions such as etherification,[19] reduction of oxygenated side groups,[8–10,14,20] and saturation of the furan ring.[21] However, DMF bears a structural similarity to its oxygenated counterpart and eliminates side reactions that stem from oxygen-containing side groups. Therefore, DMF can serve as a model compound to understand the ring-opening chemistry.

Herein, we present a combined experimental and computational study on the reaction network of DMF over Ru/C in the

[a] M. J. Gilkey, A. V. Mironenko, L. Yang, Prof. D. G. Vlachos, Prof. B. Xu
Catalysis Center for Energy Innovation
Department of Chemical and Biomolecular Engineering
University of Delaware
Newark, Delaware 19716 (United States)
E-mail: vlachos@udel.edu
bxu@udel.edu

Supporting Information and the ORCID identification number(s) for the author(s) of this article can be found under http://dx.doi.org/10.1002/cssc.201600681.

© 2016 Wiley-VCH Verlag GmbH & Co. KGaA, Weinheim

presence of 2-propanol as a hydrogen donor through catalytic transfer hydrogenation (CTH).[22] We show that the dominant pathways involve either ring-saturation or ring-opening, which occur in parallel. By extension, we show that oxygenated furanic species 5-methylfurfural (MFL) and (5-methyl-2-furyl)methanol (MFA) undergo reduction to DMF before ring-opening over Ru/C rather than direct ring-opening from the oxygenated furan. We hypothesize that the DMF ring-opening chemistry proceeds via common, surface-adsorbed, ring-opened intermediates.[23]

Results and Discussion

Reaction network of DMF HDO over Ru/C

The HDO of DMF shows two dominant pathways: ring-saturation and ring-opening (Scheme 1 a). After 2 h, nearly all DMF is consumed (~97% conversion) to form the ring-saturated species 2,5-dimethyltetrahydrofuran (DMTHF) as the main product (~73%) and the ring-opened products 2-hexanol (HOL; ~19%) and 2-hexanone (HON; ~1%; Figure 1 a). The high carbon balance (>95%) suggests that no other major product is present. Control experiments with each of the main products (DMTHF, HOL, and HON) as a starting substrate suggest that ring-opening and ring-saturation likely occur as parallel rather than sequential reactions. If DMTHF was used as the starting material under identical reaction conditions, ring-opening was negligible and only a trace amount of HOL (<1%) was observed (Table 1, entry 5). This indicates that DMTHF is not an intermediate in ring-opening to HOL. Similarly, HOL and HON do not ring-close, which further indicates that ring-opening and ring-saturation are parallel pathways. The hydrogenation of HON to HOL occurs favorably with a conversion of 93% (95% selectivity; Table 1, entry 3), whereas the dehydrogenation of

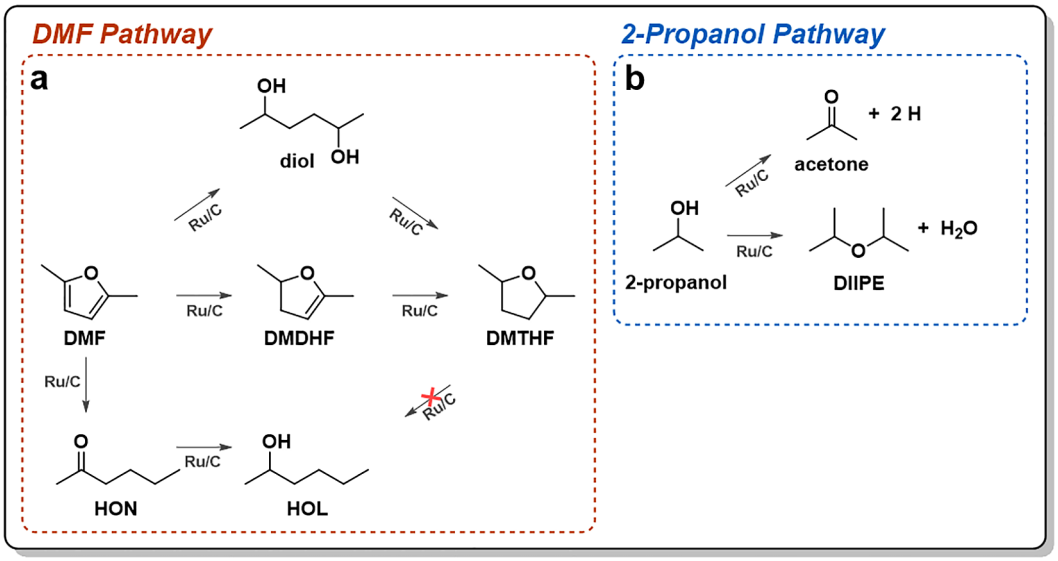

Scheme 1. Reaction networks of Ru/C-catalyzed CTH of a) DMF and b) 2-propanol.

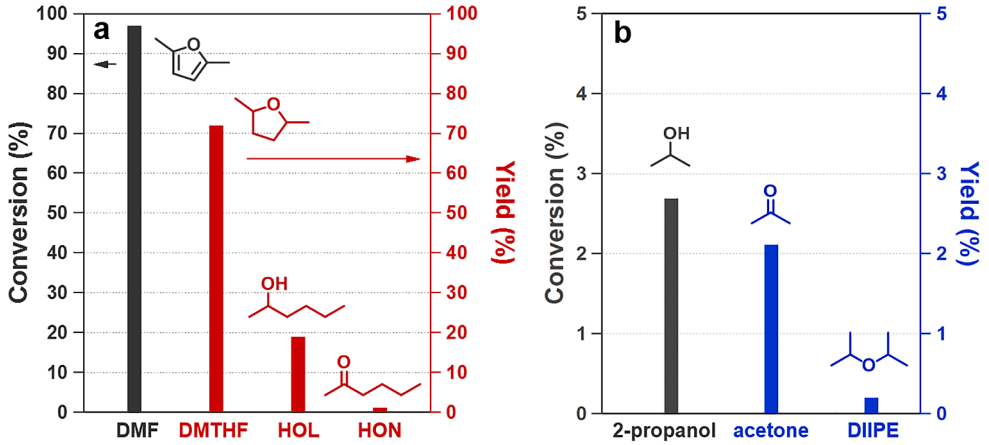

Figure 1. Product distribution for a) DMF hydrogenation and b) 2-propanol dehydrogenation. Conditions: 1 wt% DMF in 14 mL 2-propanol, $T=80\,^{\circ}C$, $t=2$ h, 80 mg Ru/C, $P_{N_2}=300$ psig.

© 2016 Wiley-VCH Verlag GmbH & Co. KGaA, Weinheim

Table 1. Reactivity and product distribution with various reactants and catalysts.

Reactant[a]	Catalyst	T [°C]	t [h]	Conversion [%]	Yield [%] HON	HOL	HDN	DMTHF	DMDHF	HDL
DMF	Ru/C	80	2	99	1.3	19	0	73	0	0
DMF	Ru/C	55	2	24	1.6	1.5	0	7.7	3.8	1.5
HON	Ru/C	80	2	98	N/A	97	0	0	0	0
HOL	Ru/C	80	2	1.4	trace	N/A	0	0	0	0
DMTHF	Ru/C	80	2	NR[b]	-	–	–	–	–	–
HDL	Ru/C	80	2	76	74	1.8	0	0	trace	N/A
HDL	Ru/C	55	2	5.5	0	0	0	3.6	0	N/A
DMF	activated carbon	80	2	NR[b]	–	–	–	–	–	–
DMF	Water	80	2	NR[b]	–	–	–	–	–	–
MFL	Ru/C	180	24	100	2.5	16	0	41	0	0
MFA	Ru/C	180	8	100	1.3	14.4	0	52	0	0

[a] DMF = 2,5-dimethylfuran, HON = 2-hexanone, HOL = 2-hexanol, DMTHF = 2,5-dimethyltetrahydrofuran, HDL = 2,5-hexanediol, MFL = 5-methylfurfural, MFA = (5-methyl-2-furyl)methanol, DMDHF = 2,5-dimethyl-2,3-dihydrofuran. [b] NR = no reaction.

HOL to HON is negligible (Table 1, entry 4). This suggests that HON could be a reaction intermediate in HOL production.

2-Propanol acts as the hydrogen donor in the Ru-catalyzed dehydrogenation to acetone and provides two hydrogen atoms to drive DMF hydrogenation (Scheme 1 b). In the absence of catalyst, no DMF hydrogenation activity occurred (Table 1, entry 8). Aside from dehydrogenation, the etherification of 2-propanol to diisopropyl ether (DIIPE) occurs. A conversion of ~3% of 2-propanol with roughly 80% selectivity to acetone and ~7% selectivity to DIIPE were observed (Figure 1 b). Hydrogenation reactions (Figure 1 a) consume roughly 77% of the produced hydrogen, calculated from the amounts of acetone and hydrogenated products formed.

As DMF converts completely at 80 °C within 2 h, a lower reaction temperature was used (55 °C) to better understand the reaction network (Figure 2 a). At this lower temperature, two reaction intermediates were revealed, namely, 2,5-dimethyl-2,3-dihydrofuran (DMDHF) and 2,5-hexanediol (2,5-HDL). After 1 h, the yields of all products increase simultaneously, which supports the hypothesis that the products are produced in parallel. The concentration of DMDHF was below the detection limit throughout the reaction at 80 °C, which is likely because of the fast hydrogenation of DMDHF to DMTHF. As the DMF hydrolysis product, that is, 2,5-hexanedione, is not observed, 2,5-HDL is formed through one of two pathways: hydrolysis of DMF followed by hydrogenation, in which the rate of hydrogenation is much faster than that of hydrolysis, or hydrolysis of an adsorbed precursor to DMTHF. Neither water in the absence of catalyst nor water in the presence of activated carbon is able to catalyze the hydrolysis reaction to 2,5-HDL at 80 °C (Table 1), which suggests that Ru sites are essential to 2,5-HDL formation. It has been proposed that water can create surface hydroxyl species, for example, $Ru(OH)_x$,[24] which might facilitate 2,5-HDL formation. An increased water concentration in the initial reaction mixture enhances the rate of 2,5-HDL formation and its accumulation (Figure 2 b). Without added water, no 2,5-HDL was observed at 80 °C, but an increase of the water/DMF molar ratio to 20 increases the 2,5-HDL yield to 55%. 2,5-HDL is not observed at higher temperatures without the addition of water because of intramolecular etherification (cyclization) to form DMTHF. This hypothesis is supported by the enhanced DMTHF yield observed by reacting 2,5-HDL on Ru/C from ~22% at 55 °C to ~74% at 80 °C (Figure 3 a). Moreover, 2,5-HDL was converted slowly to DMTHF on Ru/C over 10 h at 55 °C (Figure 3 b).

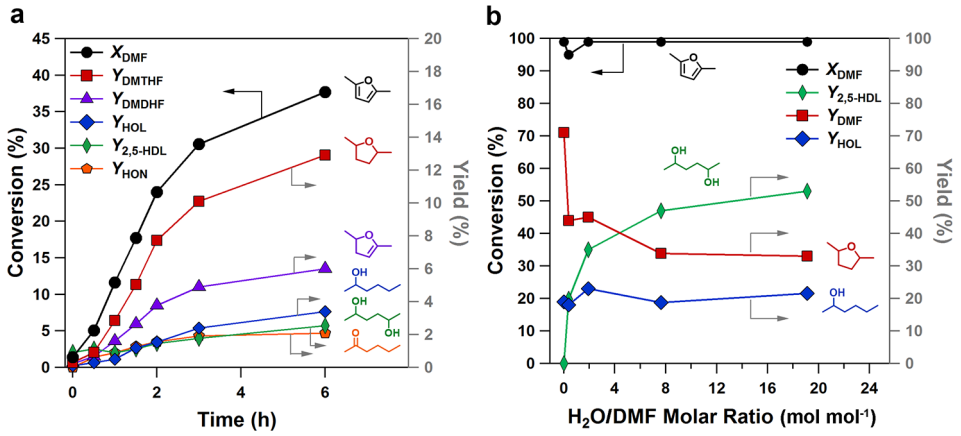

Figure 2. a) DMF conversion and major species yields versus time at 55 °C and b) effect of water on product distribution at 80 °C. Arrows point to the appropriate axis. Reaction conditions: 1 wt% DMF in 14 mL 2-propanol, $m_{cat.}$ = 80 mg reduced Ru/C, P_{N_2} = 300 psig, t = 2 h.

© 2016 Wiley-VCH Verlag GmbH & Co. KGaA, Weinheim

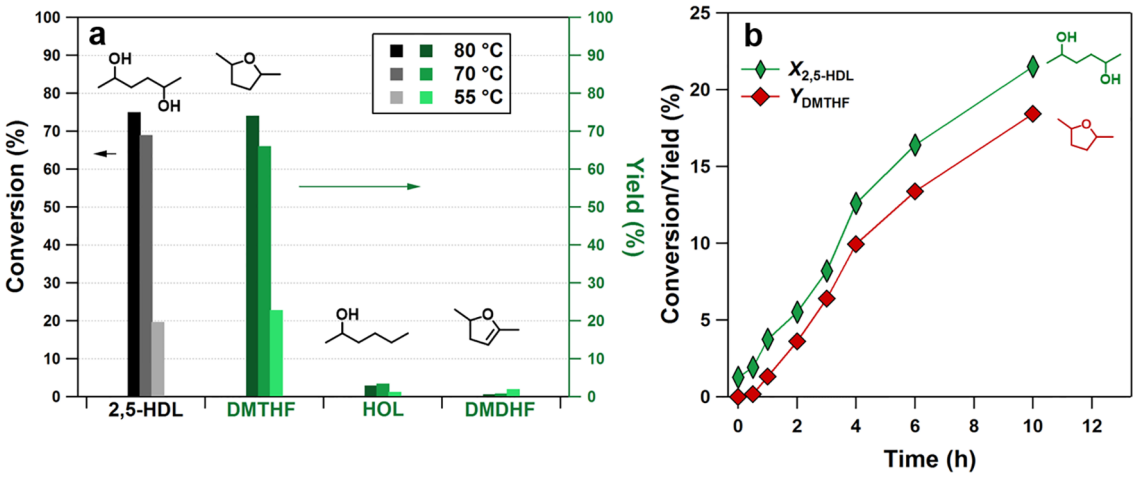

Figure 3. 2,5-HDL activity. a) Product distribution at 55, 70, and 80 °C after 2 h and b) a transient profile at 55 °C that shows that only DMTHF arises as a major product over time. Reaction conditions: 1 wt% HDL in 2-propanol, $m_{cat.}$ = 100 mg Ru/C, t = 2 h, P_{N_2} = 300 psig.

Theoretical insights into DMF reaction pathways on Ru/C

DFT calculations and microkinetic modeling help to elucidate energetics, structures, and surface coverages of reaction intermediates. Our previous work has shown that 2-methylfuran (MF) undergoes ring activation on Ru surfaces by isotopic labeling and mass fragmentation analysis.[23] Once coordinated to the Ru surface, the furan ring of MF is susceptible to reversible ring-opening and closure, and deuterium can be added to the unprotected α-carbon atom. The co-adsorbed solvent plays a crucial role in the energetics of surface reactions and explains the reactivity trends. As DMF bears a structural similarity to MF and exhibits a similar interaction with the Ru surface, we combined DFT and microkinetic modeling to elucidate the elementary processes of DMF ring-opening and hydrogenation and accounts for the presence of 2-propanol.

Microkinetic modeling reveals that for a DMF and 2-propanol reaction mixture (same composition as used in the reactivity study) on Ru(0001), three species are dominant: 2-propoxy (~0.67 monolayers, ML), open-ring form of DMF (~0.29 ML), and 2-propanol (~0.03 ML). Accordingly, all DFT calculations were performed in the presence of co-adsorbed 2-propoxy (0.75 ML) to emulate the surface/solvent environment (Figure S4). In the first step, DMF adsorbs on the surface in the flat conformation with a binding energy of −0.7 eV (Scheme 2, species **1 a**; Table S1, reaction 1). On a crowded surface, the adsorption is much less exothermic compared to that on a pristine Ru(0001) (−2.1 eV) because of steric repulsive interactions with 2-propoxy. The ring-opening barrier in the adsorbed DMF is low (0.4 and 0.6 eV on a crowded and pristine surface, respectively; Table S1, reaction 5), and the reaction is exothermic (−0.7 and −0.4 eV in the presence and absence of 2-propoxy,

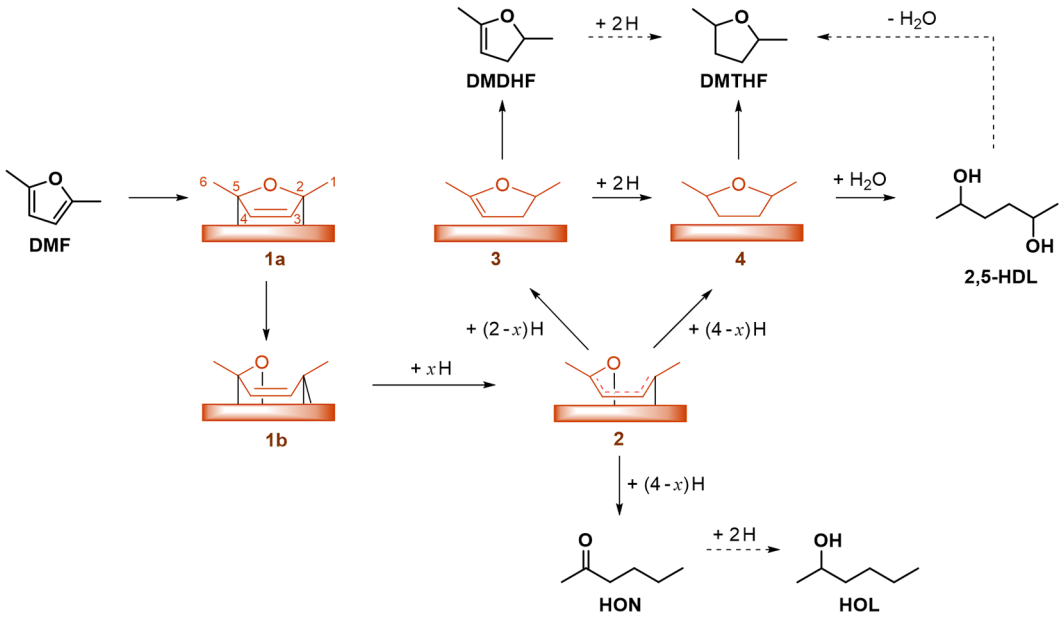

Scheme 2. Proposed DMF hydrogenation mechanism. Species drawn in black are bulk species and those drawn in orange are adsorbed to the Ru surface.

© 2016 Wiley-VCH Verlag GmbH & Co. KGaA, Weinheim

respectively). Consequently, DMF is present primarily as an open-ring structure on the surface (Scheme 2, species **1 b**), as indicated by the microkinetic model (coverages are displayed in Figure S3). Previously,[23] we found that in the open-ring MF intermediate, H addition at the α-C position exhibits a barrier comparable to that in the closed-ring state (1.1–1.3 vs. 1.0 eV on pristine Ru(0001)). As the coverage of the closed-ring DMF is negligible ($< 10^{-12}$ ML), we propose that the subsequent hydrogenation occurs predominantly via the open-ring DMF intermediate **1 b**.

DMTHF is likely formed by the ring closure of partially hydrogenated surface intermediates. Although ring-closing is difficult in the open-ring DMF (1.0 eV barrier, 0.7 eV reaction energy based on microscopic reversibility; Table S1, reverse reaction of reaction 5), calculations indicate that ring-closing becomes more facile with the increasing degree of hydrogenation. For example, ring-closing to form α-C-monodehydrogenated DMTHF is exothermic (−0.3 eV) and exhibits a low barrier (0.6 eV; Table S1, reaction 6). Consequently, partially hydrogenated open-ring intermediates **2** form their closed-ring counterparts **3** and **4** easily (provided that the α-C is not fully saturated),[25] which leads to DMTHF as a dominant product, in agreement with experiments. Interestingly, both open-ring DMF and monodehydrogenated DMTHF exhibit similar ring-closing energetics on a pristine Ru(0001) surface (0.9 and 0.8 eV barriers and 0.4 and 0.3 eV reaction energies, respectively; Table S1, reactions 5 and 6). Therefore, differences in the ring-closing energetics of open-ring DMF and monodehydrogenated DMTHF on a crowded surface can be attributed entirely to steric interactions with co-adsorbed 2-propoxy. The experimental observation of DMDHF suggests that the ring-closing step likely becomes favorable following the double hydrogenation of the open-ring DMF at the α-C and β-C positions to form **2**. Subsequent hydrogenation of the double bond in **2** (C_4–C_5 bond) results in surface-adsorbed DMTHF (**4**), which then desorbs (0.6 eV desorption energy; Table S1, reaction 3). All calculated reaction energies and barriers are summarized in Figure 4.

The detailed mechanistic steps the open-ring DMF (**1 b**) hydrogenation towards HON and HOL depend on the relative rates of C–H versus O–H bond formation. If the O–H bond formation is facile, hydroxyl-containing intermediates would form early in the reaction sequence, and HON will not form. As a result of the high oxophilicity of Ru, however, DFT calculations indicate that reactions that involve O–H bond formation typically exhibit higher barriers than those for the C–H bond formation, and thus should occur late in the reaction sequence.[23] For example, we found the C–H formation barrier in the acetone-to-2-propoxy transformation to be 0.6 eV, which is much lower than 1.3 eV for the subsequent O–H formation step. Similar conclusions have been reached by Sinha and Neurock for the hydrogenation of C_1–C_4 aldehydes and ketones on Ru(0001).[26] As a result of the high O–H bond formation barrier, it is likely that hydrogen atoms will saturate all C atoms before O and the 2-hexoxy intermediate will form, which leads to both HON and HOL, consistent with experiments.

As indicated by the experimental data, 2,5-HDL also forms in the presence of water over Ru/C, possibly by the hydrolysis of species **4** from adsorbed hydroxyl groups or bulk-phase water. We only considered the former possibility in our calculations because the amount of water formed in the reactions is insignificant. This is supported by the product distribution as a function of reaction time, which shows the simultaneous production of ring-saturated and ring-opened products at low temperatures. In addition, it is consistent with a mechanism proposed previously that shows ring activation of alkylated furanics on Ru surfaces.[23] At higher temperatures (80 °C) and longer times, DMDHF and HON are consumed by further hydrogenation reactions (Figure 1; Table 1, entry 3) and 2,5-HDL is consumed by etherification (Figure 3).

Effect of the side group

The ring-opening of DMF paves the way to understand the ring-opening of other furanic compounds. To assess the ring-

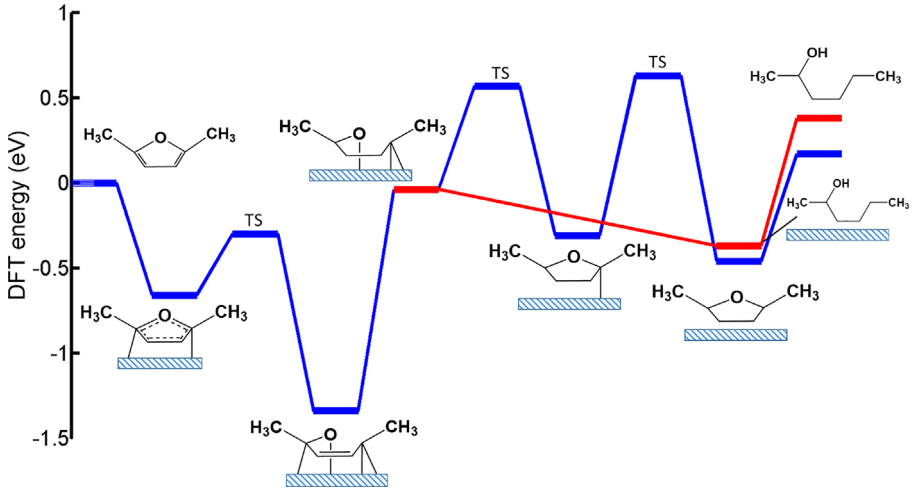

Figure 4. DFT-derived energy pathways that connect the reactant (DMF) and two products (DMTHF, blue; 2-hexanol, red). Selected reaction steps are shown. The energy diagram is based on the energetics reported in Table S1. The balance surface H atoms are not displayed. Transition states are marked as TS.

© 2016 Wiley-VCH Verlag GmbH & Co. KGaA, Weinheim

opening of similar oxygenated furanics, we employed 5-methylfurfural (MFL) and (5-methyl-2-furyl)methanol (MFA) as reactants, which bear a structural similarity to DMF and process a carbonyl and a hydroxymethyl group, respectively, instead of a methyl group. The presence of oxygen-containing side groups in MFL and MFA expands the reaction network. Ring-opening and hydrogenation reactions from MFL and MFA can result in either 1,5-hexanediol or 1,2-hexanediol, which depends on the preferential C–O cleavage on Ru/C (Scheme 3, red box). However, various other reactions can also occur, which include the decarbonylation to MF from MFL, reduction of substitutional side groups to DMF, ring-saturation to MTHFA, or etherification reactions to MFE (Scheme 3).

At 170 °C, Ru/C catalyzes the reduction of the oxygenated side group in MFL or MFA selectively to DMF rather than the hydrogenation and hydrogenolysis of the furan ring to 1,2- or 1,5-HDL (Figure 5). Time-dependent product distribution data with MFA as the reactant indicate that etherification to 2-methyl-5-[(1-methylethoxy)methyl]furan (MFE) occurs before C–O bond scission of the side group to DMF at short times (Figure 5 a), which is attributed to the high concentration of solvent molecules. Following the hydrogenolysis of MFA (or MFE) to DMF, ring-saturation to DMTHF and ring-opening to HON and HOL occur, in agreement with the proposed reaction pathway from DMF. In addition, the ratio of DMTHF to HOL formed from the cascade reaction from MFA is 2.6. This is lower than that if DMF is used as a starting material at 80 °C (~4; Figure 1 a); however, the temperature used if MFA is used as the starting material (170 °C) is much higher, which suggests that higher temperatures might favor ring-opening over ring-saturation. The carbon balance throughout the course of the reaction never exceeds 85 %, and decreases to below 70 % after 4 h. This is likely because of the production of ethers and oligomers at high surface coverages of MFA and MFE. The de-etherification reaction starts to outweigh etherification after 1 h, which is likely driven by DMF formation. A carbon balance of 73 % is found after 8 h of reaction. MFL kinetic data at 200 °C parallel that of MFA closely, wherein DMTHF and HOL/

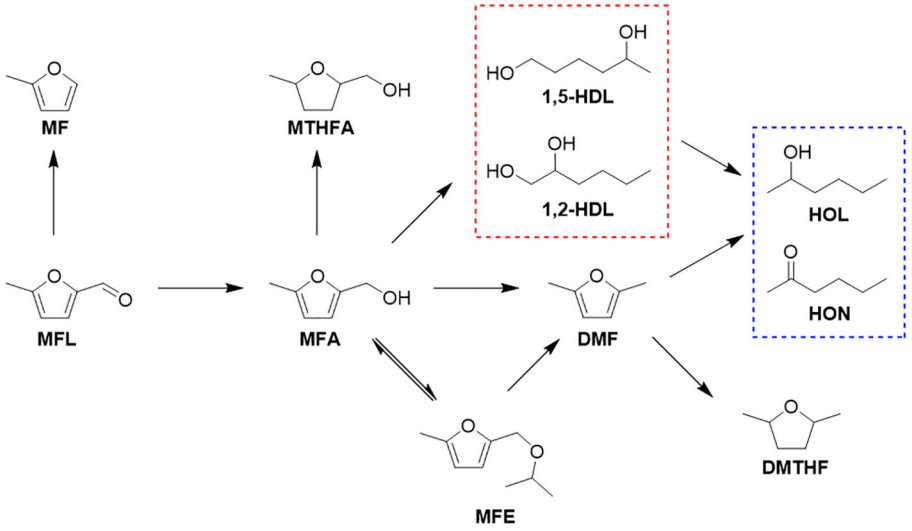

Scheme 3. Possible pathways from MFR and MFA including decarbonylation, etherification, hydrogenation, and hydrogenolysis. The red box denotes ring-opened products from oxygenated furanics (diols), and the blue box denotes those from reduced furanics, for example, DMF.

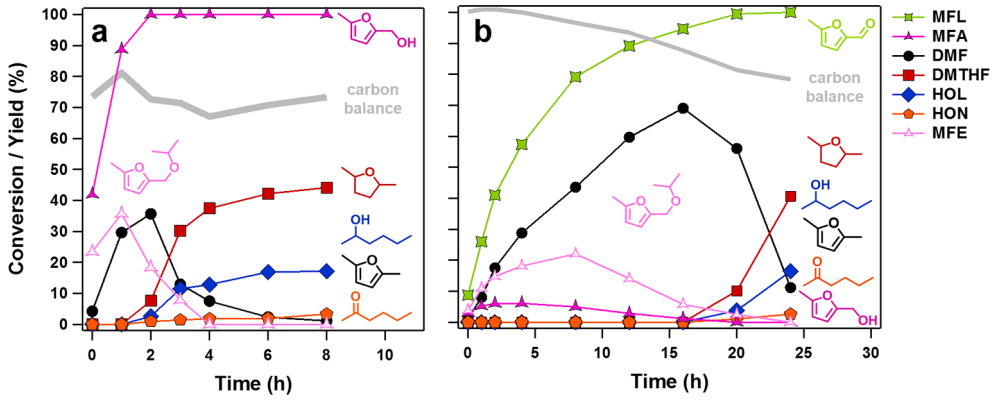

Figure 5. Transient profiles of a) MFA HDO at 170 °C and b) MFL HDO at 200 °C, which show the reduction of oxygenated substitutional groups before the ring-opening of DMF. Reaction conditions: 1 wt % reactant in 100 mL 2-propanol, P_{N_2} = 300 psig, $m_{cat.}$ = 500 mg.

© 2016 Wiley-VCH Verlag GmbH & Co. KGaA, Weinheim

HON are the final products observed following the reduction of the carbonyl group in MFL (Figure 5b). Following hydrogenation to form MFA, hydrogenolysis to DMF occurs, from which either ring-opening to HOL or ring-saturation to DMTHF proceeds. The DMTHF and HOL selectivities are nearly identical to those if MFA is used as the starting material (~2.5), which is consistent with the observation that MFA is a common intermediate for all products from MFL. The carbon balance in the reaction with MFL decreases steadily throughout the course of the reaction. This might, again, be attributed to oligomerization or polymerization reactions from MFA,[24] DMF,[27] or both. A higher carbon balance throughout the course of the reaction from MFL might be attributed to the propensity of furanic compounds with a $-CH_2OH$ side group to polymerize compared to those with a carbonyl group. For example, furfuryl alcohol is more prone to polymerization than furfural.[28]

DMF is the common intermediate in the HDO of oxygenated furanic compounds over Ru/C, which could be attributed to the oxophilic nature of Ru. This is consistent with previous studies in which high yields to DMF from HMF and to MF from furfural were achieved on catalysts with oxophilic metals.[6,9,29,30] The preferential reduction of side groups, rather than the furan ring, is likely because of the strong interaction of oxygen-containing groups with the oxophilic surface. Alkylated furans, for example, MF and DMF, can be further reduced through ring-opening or ring-saturation pathways, which is shown in this work and elsewhere.[30–33] In this work, the use of CTH at 80 °C resulted in a ~4:1 ratio of DMTHF to HOL at full conversion. The incorporation of molecular H_2 in place of CTH could drive changes in product selectivity, for which overhydrogenation to alkanes, for example, *n*-hexane, or C–C bond cracking to lighter hydrocarbons may occur if high-pressure H_2 is used. In addition, Wang et al. proposed that a higher surface coverage of H_2 favors ring-saturation over ring-opening because of the change of the adsorption configuration of the reaction intermediates, which suggests that the ratio of DMTHF and HOL might be influenced by H_2 pressure.[34] The preservation of oxygen-containing side groups is key in the production of valuable linear oxygenates, for example, 1,6-hexanediol, for which the selective cleavage of C–O bonds in the ring is needed. In this regard, Ru/C is a poor catalyst. Driving selectivity toward ring-opening requires bi- or multifunctional catalysts able to adsorb furanic molecules selectively through surface–ring interactions and stabilize oxygen-containing side groups. Dumesic et al.[17] reported that Rh-ReO_x catalysts can ring-open oxygenated tetrahydrofurans selectively, for example, tetrahydrofurfuryl alcohol (THFA). The ring-opening of alkylated tetrahydrofurans, for example, 2-methyltetrahydrofuran, over these bimetallic catalysts proceeds more than 20 times slower. This is in agreement with our findings that DMTHF is inactive toward ring-opening over Ru/C because of the endothermicity and energy barriers affiliated with the dehydrogenation (adsorption) and ring-opening reaction. Moreover, Brønsted acidity, introduced by ReO_x, was proposed to play a key role to protonate the oxygen in the fully hydrogenated furan ring to lead to an open-ring adsorbed intermediate. Adsorbed hydrogen on metal sites then hydrogenates the intermediate to the final product. Another proposed role of the oxide species in the ring-opening chemistry is to provide binding sites for oxygen-containing side groups, and the hydrogenated furan ring is opened on adjacent metal sites.[18,35–37] Therefore, results from the current study, along with previous work, suggest that the selective ring-opening of furanic compounds is unlikely to occur on monometallic surfaces and requires more than multiple types of active sites.

Conclusions

A combined experimental and computational investigation of the ring-opening of 2,5-dimethylfuran (DMF) and oxygenated furanic compounds on Ru catalysts was employed to map out the reaction network and energetics. With 2-propanol as the hydrogen source, ring-opening to 2-hexanone and 2-hexanol and ring-saturation to 2,5-dimethyltetrahydrofuran from DMF occur in parallel. No interconversion between the ring-opening and ring-saturation products is observed. Computations indicate that DMF adsorbs on Ru in an open-ring configuration, which is the common intermediate for the ring-opening and ring-saturation pathways. The ring-closing of partially hydrogenated open-ring species is thermodynamically favored and is aided by steric interactions with co-adsorbed 2-propoxy derived from the solvent. Experiments that started from oxygenated furanics 5-methylfurfural and (5-methyl-2-furyl)methanol show that DMF is a common reaction intermediate, which indicates that the reduction of the oxygenated substitutional groups is preferred to furan ring-opening on Ru. Our findings combined with previous results suggest that bi- or multifunctional catalysts are needed to facilitate selective ring-opening.

Experimental Section

Catalytic activity evaluation

Reactions were conducted by using a 50 mL stainless-steel pressure vessel (Parr Instruments) with magnetic stirring, and the reaction temperature was controlled by using a proportional–integral–derivative (PID) controller. Reaction solutions were made by adding 1 wt% of reactant to 14 mL of pure 2-propanol, in which 2-propanol acts as both the solvent and the hydrogen source, along with 80 mg of reduced Ru/C (5 wt% loading, Sigma Aldrich). The reactor was then sealed and purged three times with N_2 before it was pressurized to a final pressure of 300 psig (N_2; 1 psig = 68.9 mbar). The temperature of the reactor was then increased to the desired temperature and maintained for a predetermined period of time. After the reaction, the reactor was quenched in an ice bath. The catalyst was then removed by filtration, and samples were placed in a vial and stored for further analysis. Reactions with intermittent sampling were conducted by using a mechanically stirred reaction vessel (Parr Instruments, 5500 Series; 160 mL) equipped with a dip tube and a 0.20 μm filter. Solutions of 100 mL of 1 wt% of reactant were added along with 500 mg of reduced Ru/C. The reactor was sealed and pressurized as discussed above. Once the desired temperature was reached, liquid samples were collected at intermediate times over the course of the reaction, and pressure and volume changes caused by sampling were deemed negligible. Each sample was stored in a vial for further analysis. All chemicals

© 2016 Wiley-VCH Verlag GmbH & Co. KGaA, Weinheim

were purchased from Sigma Aldrich and were used without further purification.

The product distribution was analyzed by using GC (Agilent 7890 A) equipped with an HP-INNOWax capillary column (30 m × 0.25 mm id × 0.5 μm film thickness) and a flame ionization detector (FID). Response factors were determined by using solutions of neat chemicals with predetermined concentrations. Identification of the liquid phase products was performed by using GC–MS (Shimadzu QP2010 Plus) system. The GC (Shimadzu GC2010) was equipped with an HP-INNOWax capillary column (30 m × 0.25 mm id × 0.50 μm film thickness) and interfaced directly to the MS (Shimadzu QP2010 Plus). Identification of the GC–MS spectral features was accomplished by comparing the mass fragmentation pattern of the products with those in the Wiley/NIST library.

Catalyst pretreatment

Commercial Ru/C catalysts (Sigma–Aldrich, 5 wt% loading) were pretreated in a H_2/He flow (20 sccm H_2, 20 sccm He) at 300 °C for 3 h and cooled to RT before use as described previously.[29]

Computational methods

We use DFT to calculate surface reaction energetics, as implemented in the VASP code.[38–41] The projector-augmented-wave method was used to describe core electrons.[42,43] Wave functions of valence electrons were expanded in a plane wave basis set with a kinetic energy cutoff of 400 eV. Electronic density at each ionic step was determined self-consistently with an energy tolerance of 10^{-4} eV. The effects of electron exchange and correlation were modeled using the Perdew, Burke, and Ernzerhof energy functional (PBE)[44] with Grimme's dispersion correction, D3.[45] The latter was essential for a better estimation of chemisorption energies of furans.[46]

Details of lattice constant optimization are reported elsewhere.[23] Adsorbates were placed on one side of the p(4×4) four-layer Ru(0001) slab with two bottom layers fixed in their bulk positions. The 3×3×1 k-point mesh was used for the first Brillouin zone sampling. Total energies were determined using the Methfessel–Paxon method with a smearing parameter of 0.1.[47] A force tolerance value of 0.05 eV Å^{-1} was used during ionic relaxation steps. Transition states were found using the climbing-image nudged-elastic band method (CI-NEB)[48–53] with 10 images located equidistantly along the reaction pathway. All calculations were performed in the presence of 0.75 ML co-adsorbed 2-propoxy species (three 2-propoxys per (4×4) supercell), which was the dominant species on the surface according to the microkinetic model (see below). All calculated reaction energies (barriers) are reported in Table S1 and Figure S1, and the corresponding structures are displayed in Figure S2.

A microkinetic model for DMF adsorption and ring-opening in the presence of 2-propanol was set up using an in-house CHEMKIN™-based Fortran code[54,55] as described elsewhere.[56] Simulations were performed by using a batch reactor as used in the experimental studies with the same initial reaction mixture composition. The chemical potentials of liquid-phase components were calculated using ASPEN Plus®. The COSMO-SAC method was utilized to estimate activity coefficients. The 2-propoxy binding energy dependence on coverage was calculated using a piecewise linear model (Figure S3) by finite differencing the integral heats of adsorption, calculated from DFT. We assume that all 2-propanol-derived surface species experience similar lateral interactions. The model included the 2-propanol dehydrogenation to acetone (barriers/energies were taken from Ref. [23]) and the DMF ring-opening (reaction 5 in Table S1).

Acknowledgements

We acknowledge support from the Catalysis Center for Energy Innovation, an Energy Frontier Research Center funded by the U.S. Department of Energy, Office of Science, Office of Basic Energy Sciences under Award number DE-SC0001004.

Keywords: biomass · hydrogenation · reaction mechanisms · ruthenium · supported catalysts

[1] D. M. Alonso, J. Q. Bond, J. A. Dumesic, *Green Chem.* **2010**, *12*, 1493–1513.
[2] Y. Nakagawa, M. Tamura, K. Tomishige, *ACS Catal.* **2013**, *3*, 2655–2668.
[3] M. Dashtban, A. Gilbert, P. Fatehi, *RSC Adv.* **2014**, *4*, 2037–2050.
[4] B. Saha, M. M. Abu-Omar, *Green Chem.* **2014**, *16*, 24–38.
[5] S. P. Teong, G. Yi, Y. Zhang, *Green Chem.* **2014**, *16*, 2015–2026.
[6] J. Jae, W. Zheng, R. F. Lobo, D. G. Vlachos, *ChemSusChem* **2013**, *6*, 1158–1162.
[7] A. J. Kumalaputri, G. Bottari, P. M. Erne, H. J. Heeres, K. Barta, *ChemSusChem* **2014**, *7*, 2266–2275.
[8] B. Saha, C. M. Bohn, M. M. Abu-Omar, *ChemSusChem* **2014**, *7*, 3095–3101.
[9] M. J. Gilkey, P. Panagiotopoulou, A. V. Mironenko, G. R. Jenness, D. G. Vlachos, B. Xu, *ACS Catal.* **2015**, *5*, 3988–3994.
[10] T. Thananatthanachon, T. B. Rauchfuss, *Angew. Chem. Int. Ed.* **2010**, *49*, 6616–6618; *Angew. Chem.* **2010**, *122*, 6766–6768.
[11] Y. Román-Leshkov, C. J. Barrett, Z. Y. Liu, J. A. Dumesic, *Nature* **2007**, *447*, 982–985.
[12] C. Wang, H. Xu, R. Daniel, A. Ghafourian, J. M. Herreros, S. Shuai, X. Ma, *Fuel* **2013**, *103*, 200–211.
[13] A. D. Sutton, F. D. Waldie, R. Wu, M. Schlaf, L. A. Silks, 3rd, J. C. Gordon, *Nat. Chem.* **2013**, *5*, 428–432.
[14] J. Tuteja, H. Choudhary, S. Nishimura, K. Ebitani, *ChemSusChem* **2014**, *7*, 96–100.
[15] T. Buntara, I. Melián-Cabrera, Q. Tan, J. L. G. Fierro, M. Neurock, J. G. de Vries, H. J. Heeres, *Catal. Today* **2013**, *210*, 106–116.
[16] T. Buntara, S. Noel, P. H. Phua, I. Melián-Cabrera, J. G. D. Vries, H. J. Heeres, *Top. Catal.* **2012**, *55*, 612–619.
[17] M. Chia, Y. J. Pagan-Torres, D. Hibbitts, Q. Tan, H. N. Pham, A. K. Datye, M. Neurock, R. J. Davis, J. A. Dumesic, *J. Am. Chem. Soc.* **2011**, *133*, 12675–12689.
[18] K. Chen, K. Mori, H. Watanabe, Y. Nakagawa, K. Tomishige, *J. Catal.* **2012**, *294*, 171–183.
[19] J. Jae, E. Mahmoud, R. F. Lobo, D. G. Vlachos, *ChemCatChem* **2014**, *6*, 508–513.
[20] S. Sitthisa, T. Sooknoi, Y. Ma, P. B. Balbuena, D. E. Resasco, *J. Catal.* **2011**, *277*, 1–13.
[21] Y. Nakagawa, K. Takada, M. Tamura, K. Tomishige, *ACS Catal.* **2014**, *4*, 2718–2726.
[22] M. J. Gilkey, B. Xu, *ACS Catal.* **2016**, *6*, 1420–1436.
[23] A. V. Mironenko, M. J. Gilkey, P. Panagiotopoulou, G. Facas, D. G. Vlachos, B. Xu, *J. Phys. Chem. C* **2015**, *119*, 6075–6085.
[24] T. Komanoya, H. Kobayashi, K. Hara, W.-J. Chun, A. Fukuoka, *Appl. Catal. A* **2011**, *407*, 188–194.
[25] J. M. Fedeyko, R. F. Lobo, D. G. Vlachos, *Abstr. Pap. Am. Chem. Soc.* **2006**, *231*, 26-CATL.
[26] N. K. Sinha, M. Neurock, *J. Catal.* **2012**, *295*, 31–44.
[27] C.-C. Chang, S. K. Green, C. L. Williams, P. J. Dauenhauer, W. Fan, *Green Chem.* **2014**, *16*, 585–588.
[28] J.-M. Pin, N. Guigo, A. Mija, L. Vincent, N. Sbirrazzuoli, J. C. van der Waal, E. de Jong, *ACS Sustainable Chem. Eng.* **2014**, *2*, 2182–2190.
[29] P. Panagiotopoulou, D. G. Vlachos, *Appl. Catal. A* **2014**, *480*, 17–24.

© 2016 Wiley-VCH Verlag GmbH & Co. KGaA, Weinheim

[30] J. Luo, L. Arroyo-Ramírez, J. Wei, H. Yun, C. B. Murray, R. J. Gorte, *Appl. Catal. A* **2015**, *508*, 86 – 93.
[31] S. Sitthisa, W. An, D. E. Resasco, *J. Catal.* **2011**, *284*, 90 – 101.
[32] H.-Y. Zheng, Y.-L. Zhu, B.-T. Teng, Z.-Q. Bai, C.-H. Zhang, H.-W. Xiang, Y.-W. Li, *J. Mol. Catal. A* **2006**, *246*, 18 – 23.
[33] X. Kong, Y. Zhu, H. Zheng, F. Dong, Y. Zhu, Y.-W. Li, *RSC Adv.* **2014**, *4*, 60467 – 60472.
[34] S. Wang, V. Vorotnikov, D. G. Vlachos, *Green Chem.* **2014**, *16*, 736 – 747.
[35] Y. Nakagawa, K. Tomishige, *Catal. Today* **2012**, *195*, 136 – 143.
[36] B. Pholjaroen, N. Li, Y. Huang, L. Li, A. Wang, T. Zhang, *Catal. Today* **2015**, *245*, 93 – 99.
[37] K. Tomishige, M. Tamura, Y. Nakagawa, *Chem. Rec.* **2014**, *14*, 1041 – 1054.
[38] G. Kresse, J. Hafner, *Phys. Rev. B* **1993**, *47*, 558 – 561.
[39] G. Kresse, J. Hafner, *Phys. Rev. B* **1994**, *49*, 14251 – 14269.
[40] G. Kresse, J. Furthmüller, *Comput. Mater. Sci.* **1996**, *6*, 15 – 50.
[41] G. Kresse, J. Furthmüller, *Phys. Rev. B* **1996**, *54*, 11169 – 11186.
[42] P. E. Blöchl, *Phys. Rev. B* **1994**, *50*, 17953 – 17979.
[43] G. Kresse, D. Joubert, *Phys. Rev. B* **1999**, *59*, 1758 – 1775.
[44] J. P. Perdew, K. Burke, M. Ernzerhof, *Phys. Rev. Lett.* **1996**, *77*, 3865 – 3868.
[45] S. Grimme, J. Antony, S. Ehrlich, H. Krieg, *J. Chem. Phys.* **2010**, *132*, 154104.
[46] V. Vorotnikov, G. Mpourmpakis, D. G. Vlachos, *ACS Catal.* **2012**, *2*, 2496 – 2504.
[47] M. Methfessel, A. Paxton, *Phys. Rev. B* **1989**, *40*, 3616 – 3621.
[48] G. Henkelman, H. Jonsson, *J. Chem. Phys.* **2000**, *113*, 9978 – 9985.
[49] G. Henkelman, B. P. Uberuaga, H. Jónsson, *J. Chem. Phys.* **2000**, *113*, 9901 – 9904.
[50] D. Sheppard, R. Terrell, G. Henkelman, *J. Chem. Phys.* **2008**, *128*, 134106.
[51] D. Sheppard, G. Henkelman, *J. Comput. Chem.* **2011**, *32*, 1769 – 1771.
[52] D. Sheppard, P. Xiao, W. Chemelewski, D. D. Johnson, G. Henkelman, *J. Chem. Phys.* **2012**, *136*, 074103.
[53] Nudged Elastic Band Method for Finding Minimum Energy Paths of Transitions, H. Jónsson, G. Mills, K. W. Jacobsen in *Classical and Quantum Dynamics in Condensed Phase Simulations* (Eds.: B. J. Berne, G. Ciccotti, D. F. Coker), 385, World Scientific, **1998**.
[54] R. Kee, F. Rupley, J. Miller, CHEMKIN-II: A Fortran Chemical Kinetics Package for the Analysis of Gas-Phase Chemical Kinetics, Sandia National Laboratories, Albuquerque, NM, **1989**.
[55] M. E. Coltrin, R. J. Kee, F. Rupley, Surface CHEMKIN (Version 4.0): A Fortran package for analyzing heterogeneous chemical kinetics at a solid-surface—gas-phase interface, Sandia National Labs., Livermore, CA (United States), **1991**.
[56] M. A. Christiansen, D. G. Vlachos, *Appl. Catal. A* **2012**, *431*, 18 – 24.

Received: May 22, 2016
Published online on ■■ ■■, 0000

© 2016 Wiley-VCH Verlag GmbH & Co. KGaA, Weinheim

M. J. Gilkey, A. V. Mironenko, L. Yang, D. G. Vlachos, B. Xu**

■■ – ■■

Insights into the Ring-Opening of Biomass-Derived Furanics over Carbon-Supported Ruthenium

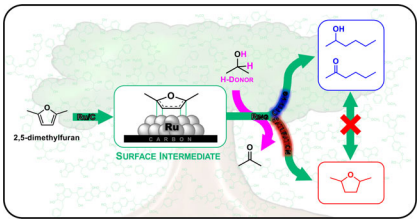

Fantastic furanics: The selective ring-opening of cellulose-derived furanic molecules is a promising pathway for the production of industrially relevant linear oxygenates. 2,5-Dimethylfuran (DMF) is employed as a model compound in a combined experimental and computational investigation to provide insights into the metal-catalyzed ring-opening. DFT calculations and microkinetic modeling indicate that DMF adsorbs on Ru in an open-ring configuration.

© 2016 Wiley-VCH Verlag GmbH & Co. KGaA, Weinheim